Pharmaceutical Research, Vol. 25, No. 7, July 2008 (© 2008)
DOI: 10.1007/s11095-008-9549-8

Research Paper

Prolonging the *In Vivo* Residence Time of Prostaglandin E_1 with Biodegradable Nanoparticles

Tsutomu Ishihara,[1,4] Miyuki Takahashi,[1] Megumu Higaki,[1] Mitsuko Takenaga,[2] Tohru Mizushima,[3] and Yutaka Mizushima[1]

Received December 14, 2007; accepted January 29, 2008; published online February 22, 2008

Purpose. Prostaglandins have potent and diverse biologic activities, but their clinical application is severely restricted, mainly due to rapid inactivation *in vivo*. In order to modulate the pharmacokinetics of prostaglandin E_1 (PGE_1), we prepared biodegradable nanoparticles as a drug carrier.
Methods. Nanoparticles encapsulating PGE_1 were prepared from a blend of poly(lactic acid) homopolymer and poly(ethylene glycol)-poly(lactide) block copolymer by the solvent diffusion method in the presence of iron.
Results. PGE_1 was efficiently and stably embedded in the nanoparticles through interaction with iron, despite being relatively hydrophilic and having unstable chemical properties. Depending on the isomers and molecular weight of poly(lactic acid) selected, PGE_1 was gradually released from the nanoparticles at various rates into diluted serum *in vitro*. Both stable retention of PGE_1 in the nanoparticles and coating of the nanoparticles with poly(ethylene glycol) led to an extremely extended blood residence time of PGE_1, as well as preferential accumulation in vascular lesions.
Conclusions. These results suggest that the present strategy is useful to advance the clinical application of PGE_1 as a therapeutic agent for vascular disorders.

KEY WORDS: iron; nanoparticle; poly(lactic acid); prostaglandin E_1; vascular disorder.

INTRODUCTION

Prostaglandin E_1 is a member of the autocoid family that has diverse and potent biologic activities in many organ systems, such as vasodilation, angiogenesis, reduction of blood pressure, inhibition of platelet aggregation, cytoprotection, and suppression of cytokine production. The discovery of these activities has led to the application of PGE_1 as a therapeutic agent for use in the treatment of chronic arteriosclerosis obliterans, peripheral vascular disease, ulcers, hepatopathy, hypertension, diabetic neuropathy, and reperfusion injury (1,2). However, there have been two major obstacles to apply PGE_1 in clinical. One is rapid inactivation of PGE_1during its first passage through the lungs (3), and another is severe side effects due to distribution to whole body. To overcome these obstacles, great efforts have been made to achieve the synthesis of chemically modified analogues that possess improved pharmacokinetics properties but share similar pharmacodynamic effects (4). Some analogues have been successfully developed, but their therapeutic application is still limited due to unanticipated side effects (5,6).

An alternative strategy consists of developing carriers for PGE_1, such as lipid emulsion (7–9), liposomes (10,11) and synthetic polymers (12,13), to modulate its pharmacokinetics. In 1983, one of the authors established a treatment technique using a lipid emulsion (so called lipid microspheres) with an average diameter of 0.2μm, which was composed of soybean oil, a drug and lecithin as the emulsifier (7). Lipid emulsion of PGE_1 (Lipo-PGE_1) is clinically used in Japan, South Korea, and China for systemic administration and shows a significantly superior clinical efficacy for peripheral vascular disease than PGE_1 clathrated in cyclodextrin (PGE_1CD: clinically used worldwide) because of its accumulation in damaged blood vessels (7,9,14). Despite enhancing the pharmacological activity of PGE_1, lipid emulsions and liposomes cannot retain PGE_1 stably under *in vivo* conditions due to their inherent structures and the relatively hydrophilic nature of PGE_1 (15,16).

On the other hand, polymeric solid particles seem to be promising carriers for the stable retention of drugs. Solid particles with a high retentiveness of PGE_1 would be expected to have the following advantages in terms of pharmacokinetics and pharmacodynamic. First, stable retention of PGE_1 by the solid particles would prevent its inactivation. Second, particles formed from biodegradable polymers such as poly(lactic/glycolic acid) (PLGA) and poly(lactic acid) (PLA), may allow PGE_1 to exhibit a long-term therapeutic effect by slow release along with degradation of the polymers (17). Third, the biodistribution of PGE_1 could be controlled by such particles

[1] DDS Institute, The Jikei University School of Medicine, 3-25-8 Nishi-shinbashi, Minato Tokyo 105-8461, Japan.
[2] Institute of Medical Science, St. Marianna University School of Medicine, 2-16-1 Sugao, Miyamae, Kawasaki Kanagawa 216-8512, Japan.
[3] Graduate School of Medical and Pharmaceutical Sciences, Kumamoto University, 5-1 Oe-honcho, Kumamoto 862-0973, Japan.
[4] To whom correspondence should be addressed. (e-mail: ishihara@jikei.ac.jp)

and specific delivery to target sites should enhance its therapeutic effects while reducing side effects. In general, colloid particles that are administered systemically undergo uptake by the mononuclear phagocyte system (MPS), resulting in accumulation in the liver and spleen. On the other hand, the pioneering work by Langer's group showed that polymeric nanoparticles (micelles) formed from poly(ethylene glycol)-block-poly(lactide) (PEG-PLA) copolymers could remain in the circulation for a prolonged period because the steric barrier of PEG chains on their surface reduced interaction with opsonins and cells of the MPS (18). Furthermore, these long-circulating nanoparticles show preferential accumulation in tumors and sites of inflammation due to the enhanced permeability and retention (EPR) effect (19,20). These nanoparticles may be an attractive carrier for delivery of PGE_1 to target sites such as vascular lesions.

In order to take advantage of these properties, it is necessary to establish a method for preparing nanoparticles with a high retentivity and high content of PGE_1. However, it is difficult to encapsulate hydrophilic drugs in solid particles although hydrophobic drugs can easily be encapsulated by hydrophobic interactions (21). Some methods (e.g. the water-in-oil-in-water solvent evaporation method) achieve the efficient encapsulation of hydrophilic drugs in larger solid particles (microparticles), but these methods generally cannot produce small nanoparticles for systemic administration (22,23). We previously reported that PLGA/PLA nanoparticles (less than 200nm in diameter) encapsulating water-soluble betamethasone phosphate with a high efficiency could be successfully prepared by an oil-in-water solvent diffusion method in the presence of zinc (24,25). We found that zinc increased the encapsulation efficiency of betamethasone phosphate in the nanoparticles by formation of a water-insoluble complex with the betamethasone phosphate (24). It was considered that this strategy of using a metal ion might also be suitable for incorporation and retention of PGE_1 in PLGA/PLA nanoparticles.

In the present study, we prepared PGE_1-encapsulated nanoparticles formed from a mixture of PEG-PLA block copolymers and PLA, and evaluated the retention of PGE_1, its release profile, and the accumulation in vascular lesions.

MATERIALS AND METHODS

Materials

Poly (D, L-lactic acid) (PDLLA) and poly (L-lactic acid) (PLLA) were supplied by Taki Chemical Co., Ltd. (Hyogo, Japan). The molecular weight of the polymers was determined by gel permeation chromatography and the composition is shown as *PDLLA* (*Mw kDa*) or *PLLA* (*Mw kDa*). Poly(ethylene glycol)-poly (D, L-lactide) (PEG-PDLLA) block copolymer was synthesized by ring-opening polymerization of D, L-lactide (Purac America, IL, USA) in the presence of monomethoxy-PEG (Mw 5200; NOF Co., Tokyo, Japan) according to the reported method (26,27). The composition and molecular weight of the block copolymers were evaluated by ^{1}H-NMR and gel permeation chromatography. PEG-PDLLA with an average Mw 14,900 was used in this study. Prostaglandin E_1 (PGE_1) was purchased from Cayman Chemical Co. and PGE_1 clathrated in cyclodextrin (PGE_1CD) was purchased from Ono Pharmaceutical Co. Ltd. (Osaka, Japan). Cy7-COOH monomer was obtained by alkali hydrolysis of Cy7-NHS ester (GE Healthcare) and subsequent HPLC purification.

Solubility of PGE_1

Crystalline PGE_1 was dissolved in ethanol at various concentrations and then the solution was added to a ninefold volume of water, 10 mM HCl aqueous solution, or phosphate-buffered saline (PBS, pH7.2). After incubation for 30 min at 25°C, the resulting solution was centrifuged at 16,000×*g* for 10 min *to precipitate insoluble PGE$_1$*. The residual PGE_1 in the supernatant was determined by HPLC with a Nova Pak-C18 column (Waters) and a UV-Vis detector (absorbance at 193 nm), using water (pH adjusted to 3.5 with acetic acid)/acetonitrile (*v*/*v* = 79:21) as the mobile phase.

To a freshly prepared aqueous solution of iron (III) chloride ($FeCl_3$) hexahydrate, various amounts of diethanolamine (DEA) were added rapidly. Next, an ethanol solution of PGE1 was added to a ninefold excess volume of the resulting solution or suspension. The final concentrations of PGE_1 and $FeCl_3$ were fixed at 0.56 and 10 mM, respectively. After incubation for 30 min at 25°C, the pH of the solutions/suspensions was monitored and then centrifugation was done at 16,000×*g* for 10 min *to precipitate insoluble PGE$_1$*. The supernatant (100 μl) was mixed with 400 μl of an aqueous citrate solution (10 mM, pH7.2), and the PGE_1 content was determined by HPLC as mentioned above.

Preparation of Nanoparticles

Nanoparticles were prepared by the oil-in-water solvent diffusion method in the presence of iron. Block copolymers, 5 mg of PGE_1, and diethanolamine (DEA) were dissolved in 525μl of acetone, while PLLA was dissolved in 225 μl of 1,4-dioxane at 50°C. The total amount of block copolymers and homopolymer was fixed at 25 mg and the blending ratio of these polymers influenced the PEG content. After mixing these solutions, iron (III) chloride anhydrous acetone solution (500 mM) was added. The resulting mixture was allowed to stand for 10 min at room temperature. To 25 ml of distilled water stirred at 1,000 rpm, the mixture was added dropwise at the rate of 48 ml/h using a 26G needle. During diffusion of the organic solvent into water, nanoparticles formed rapidly along with the solidification of PLA and the block copolymers. Immediately, 2.5 ml of aqueous 0.5M citrate solution (pH7.2) and 125 μl of aqueous 200 mg/ml Tween 80 solution were added to the resulting nanoparticle suspension to chelate iron (III) and enhance stable dispersion of the nanoparticles, respectively. Finally, the nanoparticles were purified and concentrated by ultrafiltration (Centriprep YM-50, Amicon).

Nanoparticles encapsulating dyes (rhodamine or Cy7) were prepared similarly by adding a small amount of either PLA-dye conjugate. The conjugates were synthesized by coupling the dyes with an amino group introduced into the PLA chain. One milliliter of an aqueous solution of ethylenediamine dihydrochloride (530 mg/ml) was mixed with 27 ml of DMSO containing *PDLLA(18)* (1,000 mg), 1-ethyl-3-(3-dimethylaminopropyl) carbodiimide hydrochloride (380mg), *N*-hydroxysuccinimide

(230 mg), and 4-(dimethylamino)-pyridine (270 mg), and the resulting solution was allowed to stand for 1day at room temperature. The synthesized PLA-ethylenediamine conjugate was purified by precipitation in an excess volume of water. PLA-dye conjugates were synthesized by mixing the PLA-ethylenediamine conjugate with rhodamine isothiocyanate or Cy7-NHS ester in DMSO and were purified by precipitation in an excess volume of isopropanol. The conjugates were characterized by gel permeation chromatography using TSKgel α-4000, α-3,000, and α-2500 columns (TOSOH Co., Tokyo, Japan), with DMF containing 10 mM $LiCl_2$ as the mobile phase. The amount of dye in the conjugates was determined by UV-Vis spectrometry. The conjugates used in this study contained 7.2nmol of rhodamine and 13.5nmol of Cy7 in 1 mg, respectively. Nanoparticles containing rhodamine were also formed from PLLA in the absence of block copolymers by the addition of 4.5 ml of acetone solution containing 25 mg of *PLLA (20)*, 1 mg of *PDLLA(18)*-rhodamine conjugate, 45 μmol of DEA, 5 mg of PGE_1, and 7.5μmol of iron (III) chloride to 25 ml of a 0.5% aqueous solution of Tween 80.

A lipid emulsion incorporating PGE_1 (Lipo-PGE_1) was prepared according to the published method (9). Lipo-PGE_1 with Cy7 was also prepared similarly by mixing with a small amount of Cy7-(dipalmitoyl-phosphatidylethanol amine) conjugate. The conjugate was synthesized by mixing Cy7-NHS ester, dipalmitoyl-phosphatidylethanol amine, and dimethylamino pyridine in chloroform/methanol (1/1 = *v*/*v*), and was purified by HPLC.

Characterization of Nanoparticles

The particle size and distribution were determined by the dynamic light scattering method (FPAR-1000, Otsuka Electronics, Ltd., Osaka, Japan), and the weighted average diameter was calculated by Marquadt's method.

The PGE_1 content of the nanoparticles was determined as follows. The nanoparticle suspension (50 μl) was evaporated in a vacuum centrifugal concentrator at 50°C. The dried nanoparticles were dissolved in 150 μl of 1,4-dioxane. Next, 150 μl of acetonitrile containing 9 μg of 3-phenylpropionate as an internal standard and 1,700 μl of an aqueous EDTA solution (50 mM, pH3.5) were added in this order. After 20 min, the solution was applied to a C18 reverse phase cartridge column (SepPak C18 200 mg, Waters). After washing the column with 6 ml of water, PGE_1 was eluted with 3 ml of acetonitrile, and the eluate was mixed with an equal volume of 9-anthryldiazomethane (ADAM: Funakoshi Co. Ltd.; Tokyo, Japan) in acetonitrile (0.2 mg/ml). After incubation of this mixture for 18h at 37°C, the PGE_1 content was determined by HPLC with a ZORBAX Eclipse XDB-C8 column (Agilent) and a fluorescence detector (excitation at 365 nm/emission at 412 nm).

The encapsulation efficiency of PGE_1 in the nanoparticles was defined as the ratio of the weight of PGE_1 to the total weight of PLA in the nanoparticles. Total PLA was calculated from the amount of lactic acid produced by the degradation of PLA and PEG-PLA (28). The purified nanoparticle suspension was mixed with an equal volume of 4N NaOH in water and the mixture was incubated for 18h at 50°C. After the addition of a ninefold excess of 340 mM phosphoric acid in water, the lactic acid content of the solution was determined by HPLC using an Inertsil ODS-2 column (GL Sciences Inc.) with detection at 220 nm.

Profile of PGE_1 Release from Nanoparticles

PGE_1-encapsulated nanoparticles prepared from various polymers were dispersed in a mixture of fetal bovine serum (FBS) and phosphate-buffered saline (PBS) (50% *v*/*v*, pH7.2) at a PGE_1 concentration of 100 μg/ml. After incubation at 37°C for the specified times, each suspension (100 μl) was diluted with 900 μl of 50 mM EDTA solution (pH7.0) and was centrifuged at 40,000×*g* for 30 min. After washing the precipitate with 1 ml of distilled water by centrifugation, the PGE_1 content was determined by HPLC as described above.

Interaction Between Nanoparticles and Cells

RAW 264.7 cells (a murine macrophage-like cell line) were added to an eight-well chamber plate at 1×10^5 cells per well and incubated overnight at 37°C in MEM containing 10% FBS. The cells were washed with PBS and incubated in 300 μl of fresh medium with rhodamine-encapsulated nanoparticles for 2h at 37°C. Next, the cells were washed six times with PBS and were fixed with 4% paraformaldehyde solution. After nuclear staining with diamino-phenylindole (DAPI), the cells were observed under a fluorescence microscope (IX71; Olympus Co., Tokyo, Japan).

Animal Experiments

Male Wistar rats (7weeks old, weighing 210–230 g) were obtained from SLC (Shizuoka, Japan) and were used to determine the blood concentration profile of PGE_1. The formulations of PGE_1 (nanoparticles, lipo-PGE_1, and PGE_1CD) were administered intravenously via the tail vein at a PGE_1 dose of 133 μg/kg. At designated intervals, blood was collected from the retro-orbital plexus, and then 50μl of blood was mixed with 400μl of 1,4-dioxane and subsequently with 50μl of 10 mM EDTA aqueous solution (pH7). Because PGE_1 and PLA are soluble in 1,4-dioxane, an excess of 1,4-dioxane was used to extract PGE_1 from the nanoparticles in addition to precipitating serum proteins. The mixture was agitated thoroughly and was centrifuged at 12,000rpm for 10 min. The supernatant (200 μl) was dried in a vacuum centrifugal concentrator at 50°C and then was redissolved in 50 mM Tris–HCl buffer (pH7.5) containing 9 mg/ml NaCl, 1.5 mg/ml bovine serum albumin, 1 mM $MgCl_2$, and 0.5 mM $ZnCl_2$. The PGE_1 content was determined by using a PGE_1 enzyme immunoassay kit (R&D Systems Inc., Minnesota) according to the manufacturer's protocol. As a preliminary experiment, each PGE_1 formulation was added to blood collected from a rat without any treatment and the PGE_1 content of the blood was determined by the method mentioned above. In each case, PGE_1 could be detected effectively and the values corresponded with those determined by HPLC, indicating that all PGE_1 in the blood was detectable independent of the formulation.

The accumulation of nanoparticles in vascular lesions was evaluated by *in vivo* fluorescence imaging. A rat model of peripheral vascular disease was created according to the reported method (29,30). In brief, male Wistar rats weighing

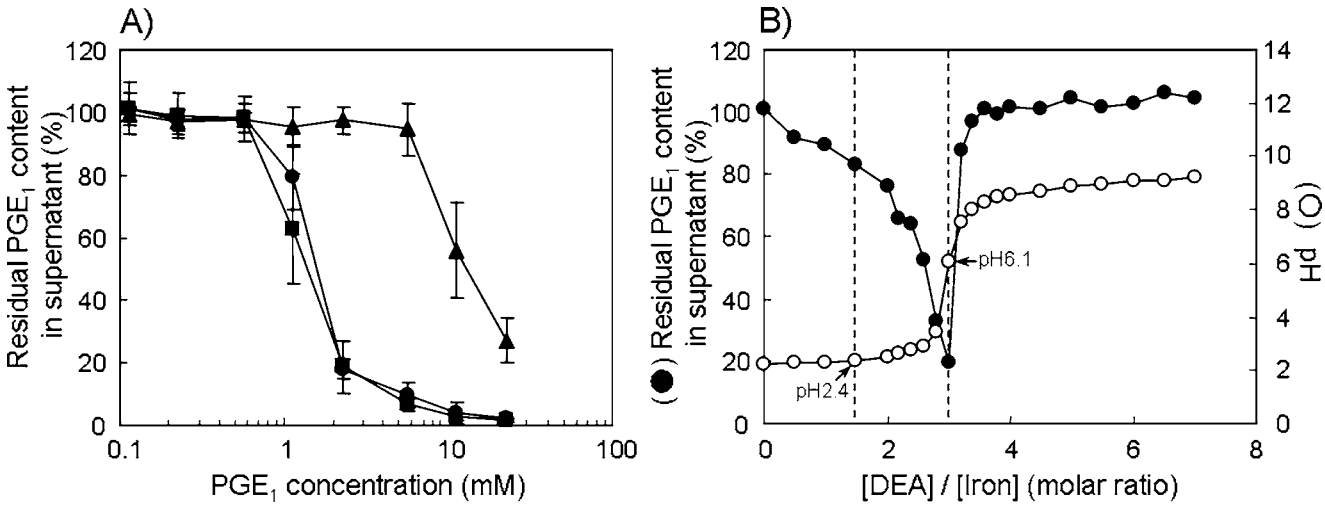

Fig. 1. Solubility of prostaglandin E_1 (PGE_1) in aqueous solutions. **A** An ethanol solution of PGE_1 with various concentrations was added to a ninefold excess volume of water (*circle*), 10 mM HCl aqueous solution (*square*), or PBS (pH 7.2) (*triangle*). After centrifugation, the residual PGE_1 in the supernatant was determined by HPLC. Each data point represents the mean±SD of three independent experiments. **B** An ethanol solution of PGE_1 was added to a ninefold excess volume of various iron (III) chloride solutions with different pH levels. The pH was adjusted by addition of diethanolamine (DEA). The final concentrations of PGE_1 and iron (III) chloride were fixed at 0.56 and 10 mM, respectively. After centrifugation, the residual PGE_1 in the supernatant was determined by HPLC.

260–280 g were anesthetized with pentobarbital (50 mg/kg, i. p.). The right femoral artery was exposed by incision and 150μl of a sodium laurate solution (5 mg/ml in 5% glucose) was injected. Next, hemostasis was achieved and the incision was sutured. After 1day, 700μl of saline containing Cy7-loaded nanoparticles, Cy7-loaded lipo-PGE_1 or Cy7-COOH monomer (each Cy7 concentration = 1.2μM) was intravenously administered via the tail vein. One day after administration, fluorescence images of the right hind paw were obtained with an *in vivo* fluorescence imaging system (eXplore Optix micro optical imager, GE Healthcare). The photon counts of the images were normalized by using the attached software. All animal experiments were performed in accordance with the Animal Experiment Guidelines of the Jikei University School of Medicine.

RESULTS AND DISCUSSION

Crystalline PGE_1 is soluble in organic solvents such as ethanol, 1,4-dioxane, DMSO, and acetone, but is only sparingly soluble in aqueous solutions. Therefore, we examined the solubility of PGE_1 in various aqueous solutions

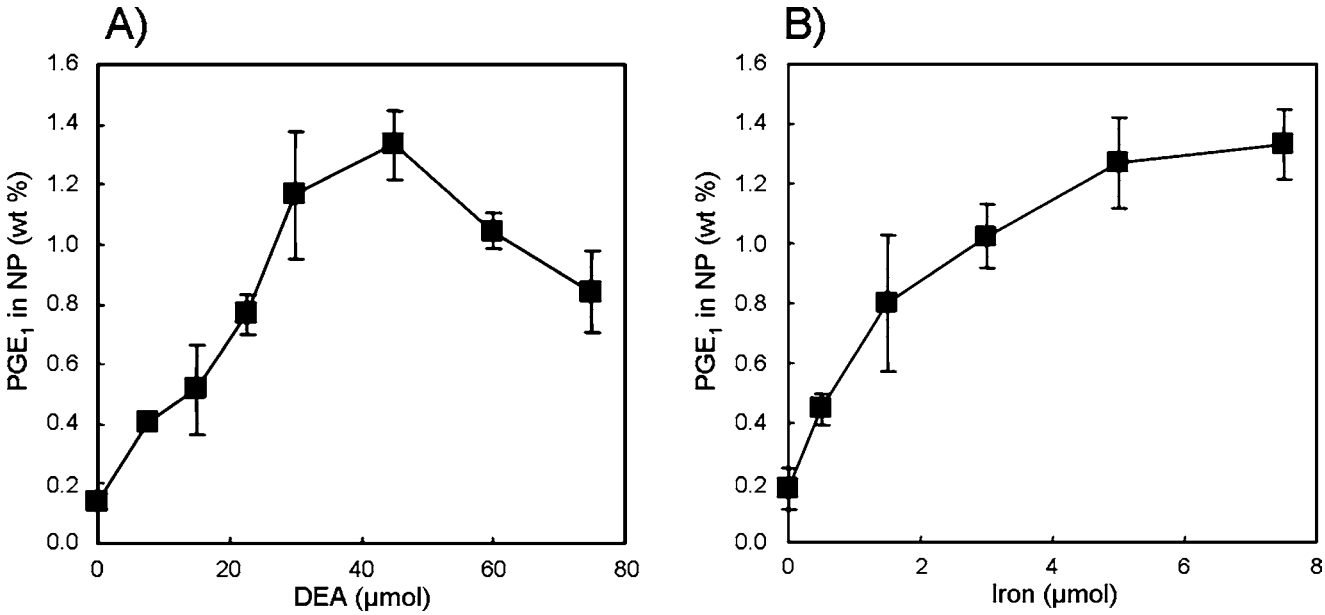

Fig. 2. Preparation of PGE_1-encapsulated nanoparticles from a blend of block copolymer and poly(lactic acid). **A** Effect of DEA on the encapsulation of PGE_1 in nanoparticles. Nanoparticles were prepared from a mixture of PEG-PDLLA and *PLLA(20)* with a 30% PEG content in the presence of 7.5 μmol iron. **B** Effect of iron and DEA on the encapsulation of PGE_1 in nanoparticles. Nanoparticles were prepared from a mixture of PEG-PDLLA and *PLLA(20)* with a 30% PEG content in the presence of DEA and iron (the molar ratio of DEA to iron was 6:1). Each data point represents the mean±SD of three independent experiments.

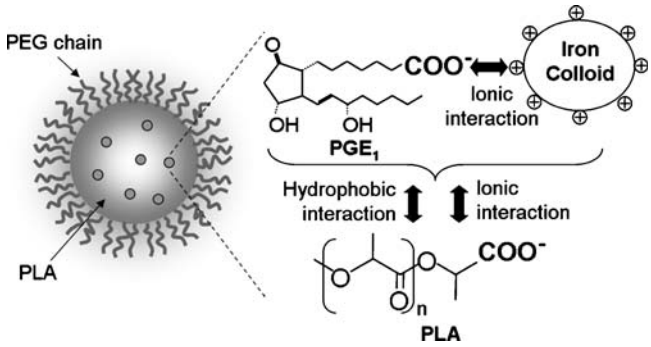

Fig. 3. Schematic illustration of nanoparticle encapsulating PGE_1.

containing 10% ethanol. The saturation limit of PGE_1 in water or a 10 mM aqueous solution of HCl was about 0.56 mM, while its solubility in PBS (pH7.2) was higher (5.6 mM) due to deprotonation of the carboxyl group (Fig. 1A). These findings indicated that PGE_1 would be soluble at a concentration of 0.56 mM in aqueous solutions, even if its carboxyl group is protonated. This level of solubility is relatively high compared with other drugs that are incorporated into solid particles (21). Although it would also depend on the method of preparation, this high solubility of PGE_1 could reduce its incorporation within solid particles. Thus, we tried to decrease the solubility of PGE_1 by formation of a complex with iron.

Iron is one of the essential minerals for life. Although iron chemistry is complicated, iron salts have been widely used in various clinical applications. The species of iron (III) chloride in aqueous solutions are conventionally classified into an unpolymerized fraction, a polymerized fraction (polymeric iron chloride produced by the hydrolysis of iron chloride), and a precipitated fraction (31,32). Although the factors that determine polymerization or subsequent precipitation are still not well understood, these processes seem to be influenced by variables such as the concentrations of iron and base, the type of base, the hydrolysis rate, mixing conditions, temperature and aging period (31,32). In an iron (III) chloride solution with a low pH, iron colloids consisting of polymeric iron chloride, iron hydroxide, or iron oxide hydroxide reach several nanometers in diameter and have a positively charged surface that can electrostatically interact with negatively charged molecules (31–33). On the other hand, at the isoelectric point (pH6–8.6), the surface charge of the colloids is neutralized and precipitates of iron colloids are preferentially formed (34). In agreement with such reports, our experiments showed the formation of colloids 5–15nm in diameter with positive zeta potentials at a low pH, while precipitates of the iron colloids formed at a high pH. Figure 1B shows the solubility of PGE_1 in 10 mM aqueous solutions of iron (III) chloride with different pH values adjusted by the addition of DEA. At a pH between 2.4 and 6.1, the residual PGE_1 content of the supernatant obtained after centrifugation of the solution gradually decreased along with the pH and the minimum content was seen at pH6.1. This indicated that electrostatic complexes were formed by PGE_1 and iron colloids along with deprotonation of the carboxyl group of PGE_1. On the other hand, at a pH lower than 2.4 and a pH higher than 6.1, most PGE_1 remained in the supernatant and did not form complexes, probably due to protonation of the carboxyl group of PGE_1 and neutralization of the positive charge of the iron colloids, respectively.

The formation of water-insoluble complexes of PGE_1 is expected to lead to its efficient incorporation into solid particles. In the present study, nanoparticles were prepared from PLA, PEG-PLA block copolymer, and PGE_1 by the solvent diffusion method in the presence of iron and DEA. In order to optimize the conditions for efficient encapsulation of PGE_1, various types of nanoparticles were prepared by altering the ratios of the additives. As shown in Fig. 1B, the amount of DEA added was crucial for formation of a water-insoluble complex of PGE_1. Therefore, the influence of the amounts of DEA and iron added on encapsulation of PGE_1 by the nanoparticles was examined. In the absence of both iron and DEA, PGE_1 was not incorporated into the nanoparticles (encapsulation efficiency was below 0.2wt%) due to its rapid diffusion out of the organic phase into the aqueous phase during the process of solidification of PLA and the block copolymer (formation of solid nanoparticles). On the other hand, in the presence of a constant amount of iron (7.5μmol), increasing the amount of DEA added led to a marked increase in the encapsulation of PGE_1 and the maximum incorporation occurred with 45μmol of DEA (Fig. 2A). In contrast, DEA could not enhance the incorporation of PGE_1 in the absence of iron. DEA probably acted to neutralize the acidic environment derived from iron chloride by its buffering effect, as shown in Fig. 1B, because similar results were also obtained when using other basic reagents (triethanolaimine and dimethylamino pyridine) instead of DEA (data not shown). These results indicated that both DEA and iron were essential for effective encapsulation of PGE_1. Furthermore, maximum incorporation of PGE_1 occurred with the addition of specific amount of DEA as well as the formation of complexes between PGE_1 and iron colloids (Fig. 1B), suggesting that PGE_1 was incorporated in the nanoparticles by the formation of complexes with iron colloids. However, maximum encapsulation of PGE_1 was

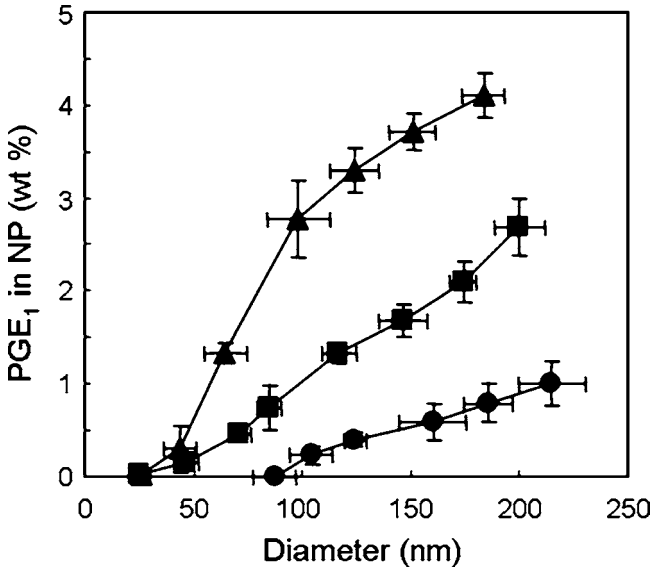

Fig. 4. Effect of the molecular weight of PLLA homopolymers on the encapsulation of PGE_1 in nanoparticles. Nanoparticles were prepared by altering the blending ratio of PEG-PDLLA and PLLA with various molecular weights [*triangle: PLLA(5)*, *square: PLLA(20)*, *circle: PLLA(33)*]. Each data point represents the mean±SD of three independent experiments.

Table I. Characteristics of Nanoparticles Formed From Various Blends of Block Copolymer and Poly(lactic acid)

Codes	PLA (Mw kDa)	Blend ratio (% of PEG content in the blend)	PGE_1 in nanoparticle (wt%)	Diameter (nm)	Polydispersity index
NP-L33	*PLLA(33)*	40	0.40±0.08	124±5	0.091
NP-L20	*PLLA(20)*	30	1.33±0.12	117±8	0.075
NP-L20s	*PLLA(20)*	45	0.47±0.06	71±5	0.051
NP-L5	*PLLA(5)*	15	3.30±0.23	124±11	0.104
NP-DL18	*PDLLA(18)*	20	1.22±0.11	121±7	0.088

*The mean (±SD) was calculated from three nanoparticle suspensions prepared independently.

observed at a DEA:iron molar ratio of 6:1, while the complex formed at a molar ratio of 3:1 (Fig. 1B). This may have occurred because excess DEA is necessary to neutralize the acidic environment induced by PLA with a terminal carboxyl group in the case of incorporating PGE_1 into nanoparticles. The encapsulation efficiency of PGE_1 also increased and almost reached a plateau along with an increase in the total amount of iron and DEA added at a constant molar ratio (DEA/iron = 6:1) (Fig. 2B). Taken together with the results shown in Fig. 2A, it was concluded that 7.5μmol of iron is adequate for efficient encapsulation of PGE_1at this scale of preparation.

Figure 3 shows the putative mechanism of PGE_1 encapsulation by nanoparticles. Deprotonated PGE_1 interacts ionically with positively charged iron colloids, at the specified pH obtained by adding DEA, resulting in the formation of a water-insoluble complex. The PGE_1 complex is efficiently incorporated by the nanoparticles through a hydrophobic interaction with PLA during the process of solidification of PLA and the block copolymers, while free PGE_1 is poorly incorporated due to its rapid diffusion into the aqueous phase (35). However, it is still unclear whether the complex formed in the organic solvent or during the process of diffusion from the organic solvent into the aqueous phase.

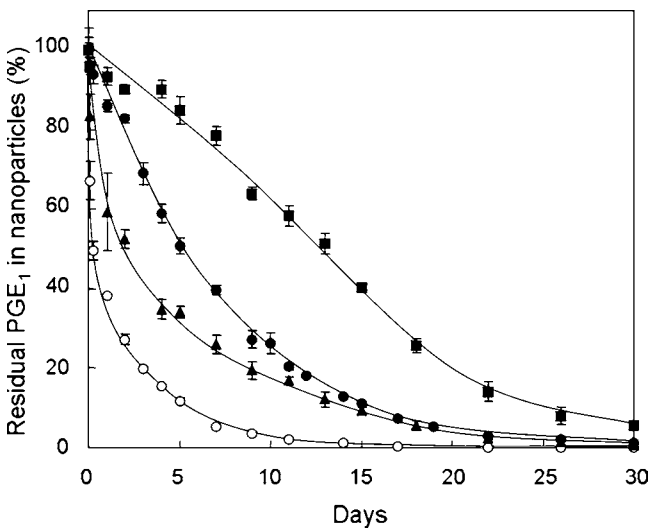

Fig. 5. Release profile of PGE_1 from nanoparticles suspended in FBS/PBS solution (50% *v/v*, pH 7.2) at 37°C. The different nanoparticles (*square: NP-L33*, *filled circle: NP-L20*, *triangle: NP-L5*, and *open circle: NP-DL18* listed in Table I) had almost the same diameter, but were formed from PLA with different compositions. Each data point represents the mean±SD of three independent experiments.

We also examined the effect of particle size and the molecular weight of PLA on encapsulation of PGE_1. Nanoparticles with various diameters were prepared by changing the blending ratio of block copolymers and PLA homopolymers with different molecular weights (Fig. 4). When block copolymers were mixed at a high ratio, there was a decrease in the diameter of the nanoparticles, indicating that the copolymers have a surfactant effect (36). The efficiency of encapsulating PGE_1 in the nanoparticles increased markedly along with particle size. This may have been because PGE_1 was more effectively retained by large particles during the process of solidification of PLA, since large particles have a smaller relative surface area compared with small particles. On the other hand, the efficiency of encapsulation increased as the molecular weight of PLA homopolymers decreased. This suggests that the PLA homopolymers acted as a reservoir of PGE_1 by ionic interaction between the residual positive charge on the PGE_1-iron colloid complex and the terminal carboxyl group of the PLA chain in addition to a hydrophobic interaction (Fig. 3), because it has been reported that cationic molecules (drugs) can be embedded in PLGA particles in a similar electrostatic manner (37).

We prepared various nanoparticles with different diameters and compositions (Table I), and then evaluated their characteristics *in vitro* and *in vivo*. In order to examine the influence of changes to the composition of PLA (such as isomers and molecular weights), four different kinds of nanoparticles (*NP-L33*, *-L20*, *-L5*, and *-DL18*) with approximately the same diameter were prepared. In addition, nanoparticles (*NP-L20 and -L20s*) with different diameters were prepared by altering the blend ratio of *PLLA(20)* and PEG-PDLLA. The release of drugs from biodegradable particles in buffered solutions is influenced by various factors such as particle diameter, composition, temperature, ionic strength, pH, and the presence of biological components. We evaluated the release of PGE_1 from nanoparticles dispersed in diluted serum (FBS/PBS 50% *v/v*, pH7.2) at 37°C (Fig. 5). It was found that the nanoparticles formed from *PDLLA(18)* (*NP-DL18*) released PGE_1 faster than those formed from *PLLA(20)* (*NP-L20*), while nanoparticles prepared from PLLA homopolymers with a lower molecular weight (*NP-L5*) tended to release PGE_1 faster than those prepared from homopolymers with a higher molecular weight (*NP-L33*), despite the similar size of these nanoparticles. Thus, nanoparticles prepared from PLLA instead of PDLLA or those prepared from PLLA with a higher molecular weight showed slower release of PGE_1. Racemic PDLLA and isotactic PLLA have different physicochemical properties (38). For example, PDLLA is an amorphous polymer, but PLLA is semi-crystalline. The glass-transition

temperature (*Tg*) of PLLA is higher than that of PDLLA, and hydrolysis of PLLA is slower. These properties also depend on the molecular weight of the polymers. Therefore, the release rate of PGE_1 might be regulated by complicated factors such as the thermodynamic stability, kinetic stability, and degradation rate of the nanoparticles. Because gradual release of PGE_1 from *NP-L33* and *NP-L20* occurred without an initial burst, this supported complete incorporation of PGE_1 into the nanoparticles rather than adsorption to the particle surface.

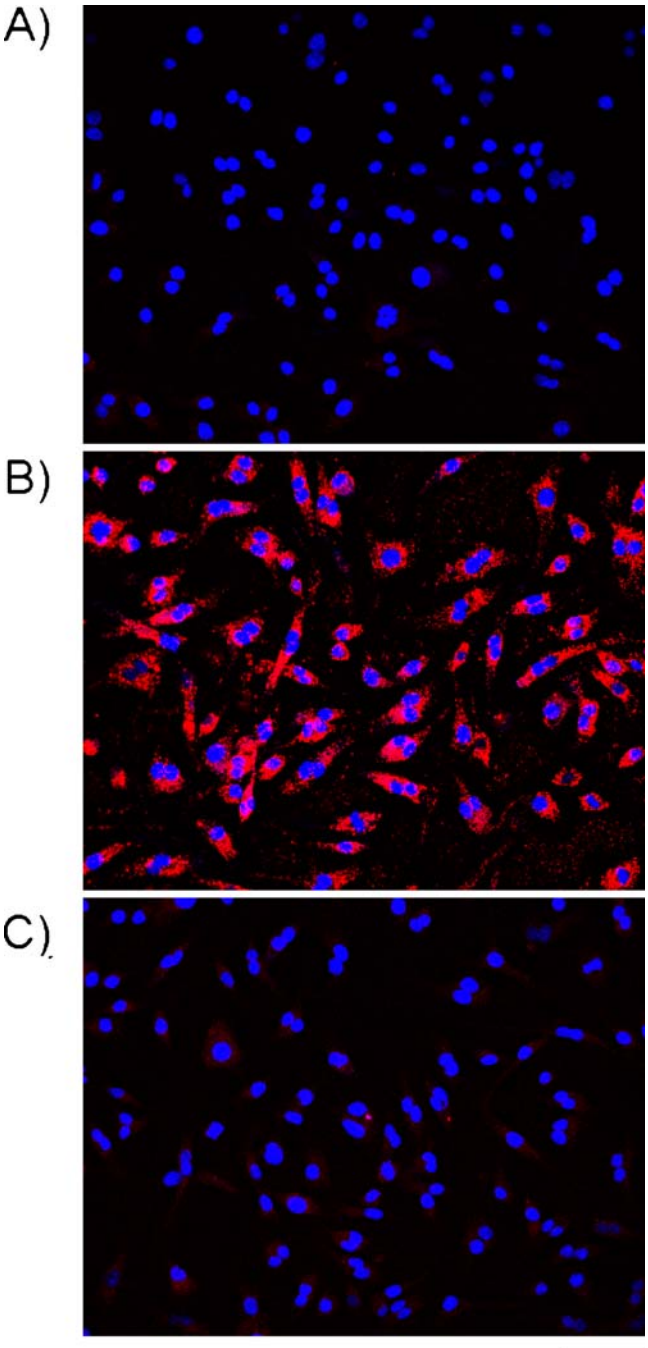

Fig. 6. Fluorescence images of RAW 264.7 cells after incubation with **A** rhodamine, **B** rhodamine-encapsulated nanoparticles prepared from *PLLA (20)* without PEG-PDLLA, and **C** rhodamine-encapsulated nanoparticles prepared with PEG-PDLLA (*NP-L20* in Table I). Blue and red images show nuclear staining by DAPI and rhodamine, respectively. Scale bar=50 μm.

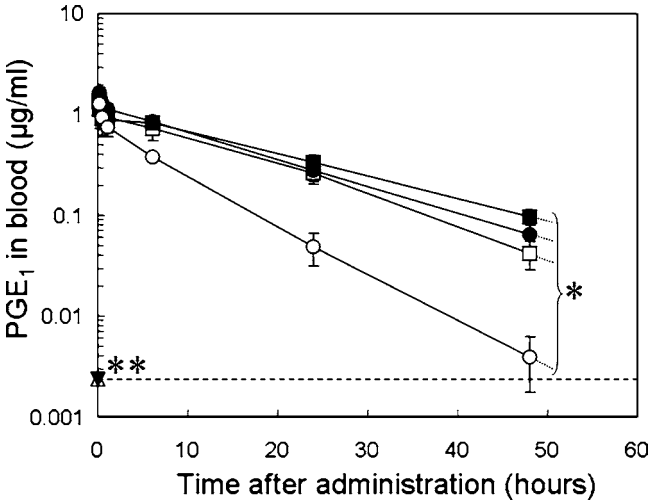

Fig. 7. Clearance of PGE_1 from the blood in rats. Various nanoparticles and other formulations incorporating PGE_1 (*triangle: Lipo-PGE_1*, *inverted triangle*: *PGE_1CD*, *filled circle*: *NP-L33*, *open square*: *NP-L20*, *filled square*: *NP-L20s*, *open circle*: *NP-DL18* in Table I) were injected intravenously at a PGE_1 dose of 133 μg/kg. Among the nanoparticles, *NP-L33*, *NP-L20*, and *NP-DL18* had approximately the same diameter, but were formed from PLA with different compositions. *NP-L20s* was formed from the same polymers as *NP-L20*, but was smaller than all the other nanoparticles. Each data point represents the mean±SD of three rats. Below the detection limit (0.0023 μg/ml) after 72 h (*asterisk*) or after 5 min (*double asterisk*).

Overall, it was demonstrated that it is possible to prepare nanoparticles with various PGE_1 release characteristics, depending on the isomers and molecular weight of the PLA homopolymers used.

Coating of particles with PEG has been reported to have a marked influence on their interaction with MPS cells both *in vitro* and *in vivo* (39). When the interaction of rhodamine-encapsulated nanoparticles with macrophage-like cells (RAW 264.7 cells) was observed by fluorescence microscopy (Fig. 6), nanoparticles made with PEG-PDLLA (*NP-L20*) showed significantly less internalization by cells (Fig. 6C) than nanoparticles which do not contain PEG (Fig. 6B), indicating sufficient masking by PEG on the surface of the nanoparticles (*NP-L20*).

Figure 7 shows the blood concentration profile of PGE_1 after intravenous administration to rats. A previous study using ^{3}H-labelled PGE_1 showed that PGE_1 was rapidly metabolized to 13,14-dihydro-15-keto-PGE_1 and that intact PGE_1 in plasma was only about 3% of the injected dose at 20 seconds after administration of Lipo-PGE_1 (40). In agreement with that result, PGE_1 was not detected by enzyme immunoassay even at 5 min after administration of Lipo-PGE_1, indicating that it leaked out from Lipo-PGE_1 into the circulation because of limited stability. After PGE_1CD (PGE_1 clathrated in cyclodextrin) was administered, there was also rapid clearance of PGE_1 due to extremely weak interaction with cyclodextrin in the blood. On the other hand, an extended residence time of PGE_1 in the blood was observed after nanoparticles (*NP-L33, -L20* , and *-L20s*) were administered (Fig. 7). Some pharmacokinetic parameters clearly displayed a significant difference between the nanoparticles and Lipo-PGE_1 (Table II). Prolonged residence of PGE_1 in the blood was based on two significant effects, which were protection of PGE_1 from

Table II. Comparative Pharmacokinetic Parameters of Various PGE_1 Formulations

	NP-L33	NP-L20	NP-L20s	NP-DL18	Lipo-PGE_1	PGE_1CD
$T_{1/2}$(h)	10.9±0.6	10.2±0.2	14.8±2.1	6.0±0.7	<0.08	<0.08
$AUC_\infty(\mu g\,h/ml)$	21.2±1.7	18.6±4.6	21.9±1.8	8.5±1.1	<0.07	<0.07
CL (ml/h kg)	6.3±0.5	7.5±2.1	6.1±0.5	15.8±2.1	>2,000	>2,000

The parameters were calculated based on the results shown in Fig. 7.
$t_{1/2}$ half-life, AUC_∞ area under the curve, *CL* total body clearance

inactivation in the lungs due to stable incorporation in the nanoparticles, and reduced interaction between the nanoparticles and cells of the MPS. When the nanoparticles were prepared from PDLLA (*NP-DL18*), PGE_1 was cleared from the blood faster than when the particles were prepared from PLLA (*NP-L33, -L20,* and *-L20s*), indicating more rapid PGE_1 release from PDLLA nanoparticles as shown in Fig. 5. Although the size of nanoparticles, as well as their surface properties, is usually an important factor in prolonging their circulation, the PLLA nanoparticles (*NP-L20*; 117nm and *NP-L20s*; 71nm) evaluated in this study exhibited little difference of residence times (Table II). Therefore, *NP-L20* with a higher PGE_1 content was used for the subsequent studies.

Longer residence of PGE_1 may not only enhance its therapeutic effects but also side effects, while rapid inactivation of PGE_1 with conventional therapeutic strategies abolishes both. However, preferential accumulation in target lesions should lead to enhancement of the therapeutic effect with minimal systemic side effects. In a rat model of peripheral vascular disease, preferential accumulation of the nanoparticles in right hind paw was observed at 1day after administration (Fig. 8), probably due to an EPR effect on circulating nanoparticles (18–20). Taken together, these results strongly suggest that nanoparticles coated with PEG may be useful for the treatment of vascular disorders such as chronic arteriosclerosis obliterans and vibration disease.

In addition, this technique for achieving the stable retention of PGE_1 in solid particles may help to advance various clinical applications of PGE_1. As shown in Fig. 6, uncoated nanoparticles were rapidly internalized by cells of the MPS. Such uncoated nanoparticles generally exhibited much higher accumulation in the liver after intravenous administration due to uptake by cells of the MPS such as Kupffer cells. Therefore, uncoated nanoparticles may be useful for the treatment of hepatopathy, fulminant viral hepatitis, and primary graft nonfunction, or for the promotion of liver regeneration. Apart from the intravenous administration of solid particles, local administration may also provide an advanced therapeutic effect. The utility of larger PLGA/PLA particles such as microspheres and implants for the control of drug release *in vivo* has been well established (21–23). Thus, local injection of such larger solid particles incorporating PGE_1 may lead to a long-term therapeutic effect at a limited location.

Finally, nanoparticles (*NP-L20*) could be successfully prepared on a large scale (30-fold scale), sterilized by filtration using a 0.2 μm membrane filter, and freeze-dried in the presence of sucrose. During storage of the freeze-dried nanoparticles for 6 months at 4°C, no chemical changes of PGE_1 or leaking (burst release) from the nanoparticles were observed. Concerning safety for clinical use, the additives in the nanoparticle formulations seem to be acceptable. PLA and PEG-PLA are desirable materials as excipients, because both are biodegradable and biocompatible, show low immunogenicity, and have little toxicity (41,42). Furthermore, iron is known to be one of the less toxic metals and some MRI contrast agents (such as Feridex® and Resovist®) with a high iron content are already being used clinically. The organic solvents that were employed (acetone and 1,4-dioxane) are harmful, but the residual content of such solvents in the nanoparticles could be decreased by ultrafiltration and freeze-drying. The residual level of solvents was sufficiently low according to the Guideline for Residual Solvents (ICH Harmonised Tripartite Guideline). Overall, our results suggest the utility of nanoparticles for various clinical applications.

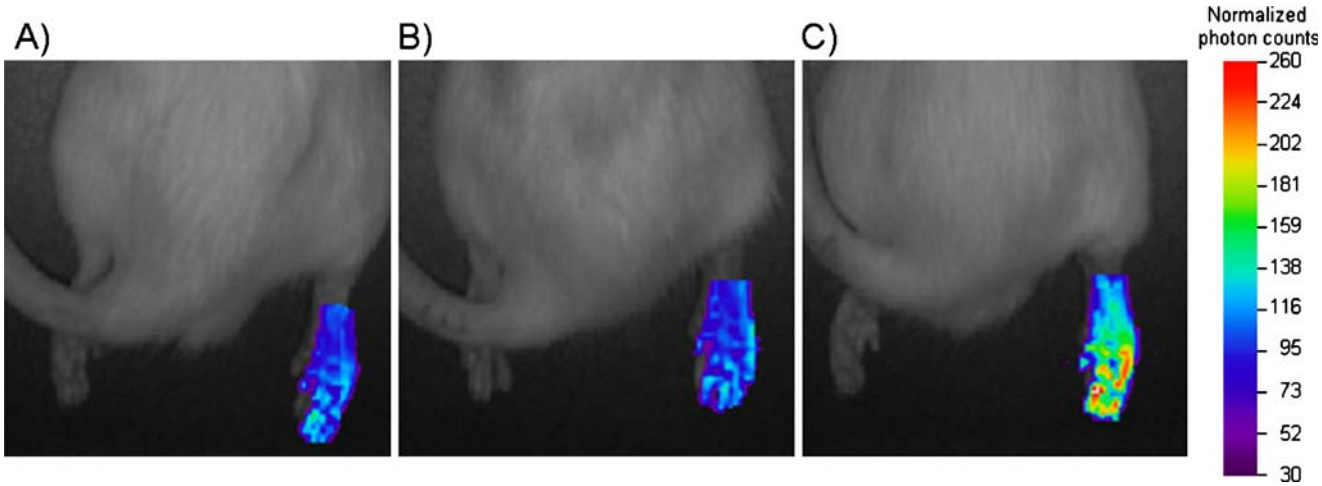

Fig. 8. Accumulation of nanoparticles containing Cy7 dye in the right hind paw in a rat model of peripheral vascular disease. Images were obtained at 1 day after intravenous administration of **A** Cy7 monomer, **B** Cy7-loaded Lipo-PGE_1, or (**C**) Cy7-loaded nanoparticles (*NP-L20* in Table I). The color bar indicates normalized photon counts derived from Cy7.

CONCLUSIONS

In conclusion, nanoparticles that efficiently incorporated PGE_1 were developed by blending PLA homopolymers and PEG-PLA block copolymers in the presence of iron. The stable retention of PGE_1 by the nanoparticles provided protection against its inactivation in the lungs, and sustained PGE_1 release could be obtained depending on the isomers and molecular weight of the PLA homopolymers. Coating of nanoparticles with PEG facilitated their accumulation in vascular lesions, suggesting the potential clinical application of nanoparticles for vascular disorders instead of Lipo-PGE_1. Use of this strategy to prolong the *in vivo* residence time and control the biodistribution of PGE_1 may open up various opportunities for clinical application.

ACKNOWLEDGEMENTS

We thank Sachiyo Shibata, Tetsushi Kubota and Yukie Tokura for their assistance with the animal experiments.

REFERENCES

1. D. M. Kerins, R. Murray, and G. A. FitzGerald. Prostacyclin and prostaglandin E1: molecular mechanisms and therapeutic utility. *Prog. Hemost. Thromb.* **10**:307–337 (1991).
2. A. Creutzig and L. Caspary. Prostanoids in therapy of peripheral arterial occlusive disease. *Therapie* **46**:241–245 (1991).
3. M. Golub, P. Zia, M. Matsuno, and R. Horton. Metabolism of prostaglandins A1 and E1 in man. *J. Clin. Invest.* **56**:1404–1410 (1975).
4. M. Bygdeman. Pharmacokinetics of prostaglandins. *Best Pract. Res. Clin. Obstet Gynaecol.* **17**:707–716 (2003).
5. G. Bianchi Porro and F. Parente. Side effects of anti-ulcer prostaglandins: an overview of the worldwide clinical experience. *Scand. J. Gastroenterol.* **24**:224–229 (1989).
6. G. Holló. The side effects of the prostaglandin analogues. *Expert Opin. Drug Saf.* **6**:45–52 (2007).
7. Y. Mizushima, A. Yanagawa, and K. Hoshi. Prostaglandin E1 is more effective, when incorporated in lipid microspheres, for treatment of peripheral vascular diseases in man. *J. Pharm. Pharmacol.* **35**:666–667 (1983).
8. Y. Mizushima. Lipo-prostaglandin preparations. *Prostaglandins Leukot. Essent. Fatty Acids* **42**:1–6 (1991).
9. T. Yamaguchi and Y. Mizushima. Lipid microspheres for drug delivery from the pharmaceutical viewpoint. *Crit. Rev. Ther. Drug Carrier Syst.* **11**:215–229 (1994).
10. D. F. Eierman, M. Yagami, S. M. Erme, S. R. Minchey, P. A. Harmon, K. J. Pratt, and A. S. Janoff. Endogenously opsonized particles divert prostanoid action from lethal to protective in models of experimental endotoxemia. *Proc. Natl. Acad. Sci. U S A* **92**:2815–2819 (1995).
11. S. Feld, G. Li, J. Amirian, P. Felli, W. K. Vaughn, M. Accad, T. R. Tolleson, C. Swenson, M. Ostro, and R. W. Smalling. Enhanced thrombolysis, reduced coronary reocclusion and limitation of infarct size with liposomal prostaglandin E1 in a canine thrombolysis model. *J. Am. Coll. Cardiol.* **24**:1382–1390 (1994).
12. H. Pan, P. Kopecková, J. Liu, D. Wang, S. C. Miller, and J. Kopecek. Stability in plasmas of various species of HPMA copolymer-PGE(1) conjugates. *Pharm Res.* **24**:2270–2280 (2007).
13. K. Akamatsu, Y. Yamasaki, M. Nishikawa, Y. Takakura, and M. Hashida. Synthesis and pharmacological activity of a novel water-soluble hepatocyte-specific polymeric prodrug of prostaglandin E(1) using lactosylated poly(L-glutamic hydrazide) as a carrier. *Biochem. Pharmacol.* **62**:1531–1536 (2001).
14. Y. Mizushima, T. Hamano, S. Haramoto, S. Kiyokawa, A. Yanagawa, K. Nakura, M. Shintome, and M. Watanabe. Distribution of lipid microspheres incorporating prostaglandin E1 to vascular lesions. *Prostaglandins Leukot. Essent. Fatty Acids* **41**:269–272 (1990).
15. S. Kawakami, C. Munakata, S. Fumoto, F. Yamashita, and M. Hashida. Targeted delivery of prostaglandin E1 to hepatocytes using galactosylated liposomes. *J. Drug Target.* **8**:137–142 (2000).
16. R. Igarashi, Y. Mizushima, M. Takenaga, K. Matsumoto, Y. Morizawa, and A. Yasuda. A stable PGE1 prodrug for targeting therapy. *J. Control. Release* **20**:37–46 (1992).
17. C. E. Astete and C. M. Sabliov. Synthesis and characterization of PLGA nanoparticles. *J. Biomater. Sci. Polym. Ed.* **17**:247–289 (2006).
18. R. Gref, Y. Minamitake, M. T. Peracchia, V. Trubetskoy, V. Torchilin, and R. Langer. Biodegradable long-circulating polymeric nanospheres. *Science* **263**:1600–1603 (1994).
19. H. Maeda, J. Wu, T. Sawa, Y. Matsumura, and K. Hori. Tumor vascular permeability and the EPR effect in macromolecular therapeutics: a review. *J. Control. Release* **65**:271–284 (2000).
20. K. Avgoustakis. Pegylated poly(lactide) and poly(lactide-co-glycolide) nanoparticles: preparation, properties and possible applications in drug delivery. *Curr. Drug Deliv.* **1**:321–333 (2004).
21. S. J. Douglas, S. S. Davis, and L. Illum. Nanoparticles in drug delivery. *Crit. Rev. Ther. Drug Carrier Syst.* **3**:233–261 (1987).
22. H. Okada and H. Toguchi. Biodegradable microspheres in drug delivery. *Crit. Rev. Ther. Drug Carrier Syst.* **12**:1–99 (1995).
23. C. E. Astete and C. M. Sabliov. Synthesis and characterization of PLGA nanoparticles. *J. Biomater. Sci. Polym. Ed.* **17**:247–289 (2006).
24. T. Ishihara, N. Izumo, M. Higaki, E. Shimada, T. Hagi, L. Mine, Y. Ogawa, and Y. Mizushima. Role of zinc in formulation of PLGA/PLA nanoparticles encapsulating betamethasone phosphate and its release profile. *J. Control. Release* **105**:68–76 (2005).
25. M. Higaki, T. Ishihara, N. Izumo, M. Takatsu, and Y. Mizushima. Treatment of experimental arthritis with poly(D, L-lactic/glycolic acid) nanoparticles encapsulating betamethasone sodium phosphate. *Ann. Rheum. Dis.* **64**:1132–1136 (2005).
26. E. Pişkin, X. Kaitian, E. B. Denkbaş, and Z. Küçükyavuz. Novel PDLLA/PEG copolymer micelles as drug carriers. *J. Biomater. Sci. Polym. Ed.* **7**:359–373 (1995).
27. T. Riley, S. Stolnik, C. R. Heald, C. D. Xiong, M. C. Garnett, L. Illum, and S. S. Davis. Physicochemical evaluation of nanoparticles assembled from poly(lactic acid)-poly(ethylene glycol) (PLA-PEG) block copolymers as drug delivery vehicles. *Langmuir* **17**:3168–3174 (2001).
28. S. Kamei, Y. Inoue, H. Okada, M. Yamada, Y. Ogawa, and H. Toguchi. New method for analysis of biodegradable polyesters by high-performance liquid chromatography after alkali hydrolysis. *Biomaterials* **13**:953–958 (1992).
29. S. Ashida, M. Ishihara, H. Ogawa, and Y. Abiko. Protective effect of ticlopidine on experimentally induced peripheral arterial occlusive disease in rats. *Thromb Res.* **18**:55–67 (1980).
30. H. Hara, H. Shimada, A. Kitajima, and Y. Tamao. Effect of (+/−)-2-(dimethylamino)-1-[[o-(m-methoxyphenethyl)phenoxy] methyl]ethyl hydrogen succinate on experimental models of peripheral obstructive disease. *Arzneimittelforschung* **41**:616–620 (1991).
31. C. M. Flynn. Hydrolysis of inorganic iron(III) salts. *Chem. Rev.* **84**:31–41 (1984).
32. T. Liu and E. S. Chian. Effect of base addition rate on the preparation of partially neutralized ferric chloride solutions. *J. Colloid Interface Sci.* **284**:542–547 (2005).
33. L. Weiss and J. R. Subjeck. The densities of colloidal iron hydroxide particles bound to microvilli and the spaces between them: studies on glutaraldehyde-fixed ehrlich ascites tumor cells. *J. Cell Sci.* **14**:215–223 (1974).
34. G. A. Parks. The isoelectric points of solid oxides, solid hydroxides, and aqueous hyrdoxo complex systems. *Chem. Rev.* **65**:177–198 (1965).
35. H. Murakami, M. Kobayashi, H. Takeuchi, and Y. Kawashima. Preparation of poly(DL-lactide-co-glycolide) nanoparticles by modified spontaneous emulsification solvent diffusion method. *Int. J. Pharm.* **187**:143–52 (1999).
36. Y. Dong and S. S. Feng. Nanoparticles of poly(D,L-lactide)/methoxy poly(ethylene glycol)-poly(D,L-lactide) blends for con-

trolled release of paclitaxel. *J. Biomed. Materials Res. A.* **78**:12–19 (2006).
37. H. Okada, M. Yamamoto, T. Heya, Y. Inoue, S. Kamei, Y. Ogawa, and H. Toguchi. Drug delivery using biodegradable microspheres. *J. Control. Release* **28**:121–129 (1994).
38. R. Jalil and J. R. Nixon. Biodegradable poly(lactic acid) and poly (lactide-co-glycolide) microcapsules: problems associated with preparative techniques and release properties. *J. Microencapsul.* **7**:297–325 (1990).
39. V. C. Mosqueira, P. Legrand, J. L. Morgat, M. Vert, E. Mysiakine, R. Gref, J. P. Devissaguet, and G. Barratt. Biodistribution of long-circulating PEG-grafted nanocapsules in mice: effects of PEG chain length and density. *Pharm Res.* **18**:1411–1419 (2001).
40. Clinical report (Kiso to Rinsho). **20**:4399–4428 (1986). (written in Japanese)
41. M. S. Shive and J. M. Anderson. Biodegradation and biocompatibility of PLA and PLGA microspheres. *Adv. Drug Deliv. Rev.* **28**:5–24 (1997).
42. J. P. Plard and D. Bazile. Comparison of the safety profiles of PLA50 and Me.PEG-PLA50 nanoparticles after single dose intravenous administration to rat. *Colloids Surf. B biointerfaces* **16**:173–183 (1999).